JOURNAL OF CATALYSIS 130, 62–75 (1991)

Surface-Enhanced Raman Spectroscopy at Transition Metal–Gas Interfaces: Adsorption and Reactions of Sulfur Dioxide on Platinum-, Rhodium-, and Ruthenium-Coated Gold

TODD WILKE,* XIAOPING GAO,† CHRISTOS G. TAKOUDIS,* AND MICHAEL J. WEAVER†

*School of Chemical Engineering and †Department of Chemistry, Purdue University, West Lafayette, Indiana 47907

Received October 11, 1990; revised February 5, 1991

Surface-enhanced Raman (SER) spectra obtained using 647-nm excitation are reported for the adsorption and oxidation of sulfur dioxide in flowing argon-based streams at ambient pressures and at 300 K on electroelectrochemically roughened gold, and on gold surfaces modified by thin (2–3 monolayer) electrodeposited films of platinum, rhodium, and ruthenium. The spectra were recorded by using a spectrograph/charge-coupled device (CCD) detector system, enabling real-time spectral sequences to be obtained within 1–2 s. Dosing with sulfur dioxide yielded a band at 1135 cm^{-1} on platinum as well as on unmodified gold, assigned to a symmetric S–O stretch of molecularly adsorbed SO_2. This band is weak on ruthenium, and absent on rhodium. A feature at 300–320 cm^{-1} is also obtained on gold, platinum, rhodium, and ruthenium, and is identified as the metal-adsorbate stretch for sulfur formed by dissociative SO_2 adsorption. On platinum and gold, oxidation of the adsorbed SO_2 requires the presence of water and CO in addition to O_2 in the feed stream. Under these conditions, the 1135-cm^{-1} feature is replaced by bands at 1010 and 1020 cm^{-1} (Pt) or 1010 cm^{-1} (Au), ascribed to adsorbed sulfate. On ruthenium, including only water and O_2 in the feed yields SO_2 oxidation to sulfate, characterized by a band at 1030 cm^{-1}. The stability of each species to temperature excursions up to 475 K is noted. Comparison is also made with potential-dependent SER spectra obtained for SO_2 at the corresponding metal-aqueous electrochemical interfaces. Similarly to the gas-phase systems, the surface oxidation as well as molecular adsorption of SO_2 can be monitored at these electrochemical interfaces with SERS. Dissociative chemisorption to yield adsorbed sulfur is strongly potential-dependent, as expected since the process is reductive. Some virtues of such parallel gas-phase and electrochemical surface spectroscopic studies are pointed out.

INTRODUCTION

Sulfur dioxide is a common by-product of combustion processes due to the oxidation of sulfur impurities present in the fuel. The catalytic oxidation of sulfur dioxide to sulfur trioxide results in the formation of sulfuric acid in the presence of water. Dissociative chemisorption of sulfur dioxide leads to adsorbed sulfur which can poison or modify the catalyst activity (*1*). Understanding the adsorption and reactions of sulfur dioxide on metal surfaces under catalytically relevant conditions is therefore of practical as well as fundamental interest.

The adsorption of sulfur dioxide on various metal surfaces has been the object of a number of studies in ultrahigh vacuum (uhv). Sulfur dioxide is observed to adsorb dissociatively on most metal surfaces, including polycrystalline nickel (*2*), iron (*3*), rhodium (110) (*4*), platinum (110) (*4, 5*), and platinum (111) (*6, 7*). The dissociation products, adsorbed oxygen and sulfur atoms, can react subsequently to form other species. Adsorbed sulfate was detected with X-ray photoelectron spectroscopy (XPS) following sulfur dioxide adsorption on nickel (*2*) and iron (*3*) surfaces. Sulfur trioxide was found to desorb from an oxidized Pt(111) surface exposed to sulfur dioxide (*6*).

Molecular adsorption of sulfur dioxide has been observed at low temperatures on gold surfaces (*2, 3*) and on the (100), (110),

0021-9517/91 $3.00

and (111) faces of silver (*8*) by using XPS and Auger spectroscopy. Vibrational studies using electron energy loss spectroscopy (EELS) have also detected molecularly adsorbed sulfur dioxide on Ag(110) (*9, 10*), Pd(100) (*11, 12*), and Cu(100) (*13*). The decomposition of adsorbed sulfur dioxide and the formation of sulfur trioxide was observed by means of EELS near 300 K on Ag(110) (*10, 14*) and Cu(100) (*13*). Adsorbed sulfate is formed above 300 K on Pd(100) exposed to sulfur dioxide (*11, 12*), while Ag(110) surfaces had to be heated to 570 K before adsorbed sulfate was observed (*10*).

The adsorption of sulfur dioxide has also been studied at atmospheric pressure on silver powders by means of surface-enhanced Raman spectroscopy (SERS) (*15–17*). Silver powders exposed to sulfur dioxide at room temperature yielded Raman bands at ca. 620 and 925 cm^{-1}, attributed to adsorbed sulfur trioxide. A band at 960 cm^{-1} was observed in the SER spectrum after a silver powder that had been dosed previously with sulfur dioxide was heated in an oxygen-containing atmosphere. This band was assigned to adsorbed sulfate formed by the oxidation of sulfur trioxide (*15*).

The SERS technique is in principle an attractive means of examining the vibrational properties of adsorbates on metal surfaces under catalytically relevant conditions since ambient or even higher gas pressures can be used without bulk-phase interferences. Such applications, however, have been limited almost entirely to silver, gold, and copper surfaces for which large Raman enhancements can be obtained with visible excitation. Nevertheless, it has recently been demonstrated in our laboratory that SERS can be extended to a range of other materials, including platinum-group metals, by electrodepositing them as thin films on a SERS-active gold substrate (*19, 20*). Silver substrates have also been utilized with some success (*21, 22*). The initial applications of such surfaces involved electrochemical systems (*19, 21*). However, we have recently demonstrated that this tactic can also be used to examine the adsorption and reactivity of NO and CO on platinum, rhodium, and ruthenium surfaces in the gas phase at ambient pressures and temperatures up to 475 K (*22*). Furthermore, the advent of charge-coupled detector technology enables SER spectra for a variety of adsorbates to be obtained sequentially on $\lesssim 1$ s timescales, allowing time-dependent surface speciation to be examined in both gas-phase and electrochemical environments (vide infra) (*22*).

Described here is the utilization of this approach to examine the adsorption and surface reactivity of sulfur dioxide at atmospheric pressure and temperatures up to 475 K on gold and platinum-, rhodium-, and ruthenium-coated gold surfaces. These surfaces were also exposed to mixtures of sulfur dioxide with oxygen and/or carbon monoxide and the effect of added water vapor was examined. In addition, the results obtained in the gas phase are compared with the corresponding SERS results obtained for sulfur dioxide on similar gold and platinum-, rhodium-, and ruthenium-coated gold surfaces in aqueous solutions, including conditions where electrochemical oxidation or reduction is taking place. A more detailed discussion of the electrochemical SERS behavior will be given elsewhere.

EXPERIMENTAL

A schematic illustration of the apparatus used in this study is provided in Ref. (*22*). The sample chamber is a stainless steel six-way cross which was operated as a continuous flow reactor at atmospheric pressure. Samples were spot-welded to a tantalum foil holder mounted on an electrical feedthrough so that the sample surface was parallel to an optical glass viewport mounted on the bottom flange of the six-way cross. The tantalum foil holder could be heated resistively by using a DC power supply, and chromel–alumel thermocouples were spot-welded to the sample edge to monitor the temperature. The gas manifold allowed the mixing of up to four gas streams; the compositions reported here are on a volume per-

cent basis. A total flow rate of 100 $cm^3\ min^{-1}$ was used and argon was utilized as a diluent. The inlet to the sample chamber directed the gas flow across the sample surface so the gas composition at the surface was virtually that of the feed. When the feed composition was changed, both the sample chamber and the manifold were evacuated by a mechanical vacuum pump to remove residual gases.

The Raman excitation source was a Spectra-Physics Model 165 Kr^+ laser operated at 647.1 nm and at a power of 20 mW on the sample. The Raman-scattered light was collected with a 50 mm diameter f/0.95 camera lens (DO Industries Model DO-5095) and focused into a SPEX Model 1877 triplemate spectrometer. The latter was equipped with a Photometrics PM512 CCD detector which was cooled to a temperature of 163 K. The detector was operated by a Photometrics CC200 camera controller which was interfaced with a Zenith 386 computer for data acquisition and storage. The spectrometer configuration utilized 600 g mm^{-1} ruled gratings in both the filter and spectrograph stage. Given the dimensions of the CCD detector, at the excitation frequency used here this arrangement limited the range of Raman frequencies that could be recorded simultaneously to about 600 cm^{-1}. Since we are interested in examining both the surface-adsorbate stretching region (150–600 cm^{-1}) and S–O vibrations (at ca. 900–1150 cm^{-1}), it was necessary to record separately spectra covering these frequency ranges. All spectra were recorded with a bandpass of 5 cm^{-1} and were obtained at room temperature unless otherwise noted.

The surfaces used in this study were 6-mm-diameter gold disks which were cut from a 0.1-mm-thick foil (99.99%, Johnson Matthey). The surfaces were mechanically polished with 1.0 and 0.3 μm alumina and then placed in a Teflon holder that exposed a region 3 mm in diameter at the center of the surface. The gold surfaces were electrochemically roughened by multiple oxidation–reduction cycles in 0.1 *M* KCl to yield SERS activity as described in Ref. (*23*). The electrodeposition of the metal overlayers utilized ca. 5×10^{-4} *M* solutions of hydrogen hexachloroplatinate(IV) ($H_2PtCl_6xH_2O$), rhodium(III) chloride trihydrate ($RhCl_3\ 3H_2O$), and ruthenium(III) chloride trihydrate ($RuCl_3\ 3H_2O$) (Aldrich). The electrolytes used were 0.5 *M* H_2SO_4 for platinum and 0.5 *M* $HClO_4$ for rhodium and ruthenium; the deposition procedures were essentially as outlined in Refs. (*19, 20*). Optimal SERS intensity was obtained with ca. 2 and 3 equivalent monolayers for platinum, and for rhodium and ruthenium, respectively. The metal overlayers were also characterized by X-ray photoelectron spectroscopy. The electron binding energies obtained for the overlayer materials are in good agreement with those measured for corresponding polycrystalline foils. Thus the Pt $4f_{7/2}$ peak was observed at 71.0 and 71.1 eV for the platinum overlayer and foil, respectively; the corresponding values for rhodium ($3d_{5/2}$ peak) are 307.1 and 307.2 eV, respectively. These measurements therefore confirm that the chemical state of the overlayer films is not altered significantly by the gold substrate. A similar conclusion was reached earlier on the basis of the electrochemical properties of the overlayer films (*19, 20*).

Electrochemical surface Raman measurements were made with a 4-mm-diameter gold disk sheathed in Teflon that was subjected to the same preparation; essentially identical voltammetric behavior was obtained for the two types of surfaces. Details of the electrochemical SERS procedures are described elsewhere (*19, 20*). All potentials quoted are with respect to the saturated calomel electrode (SCE). Anhydrous sulfur dioxide (99.98%) and oxygen (99.998%) (Matheson) were used without further purification. Hydrogen (99.99%) and argon (99.998%) (Matheson) were passed through molecular sieves and oxygen purifiers before use. Carbon monoxide (99.8%) was obtained from Matheson in an aluminum cylinder that was filled at the source to eliminate the presence of iron carbonyls.

RESULTS

Unmodified Gold

After a sample was mounted in a reactor, the chamber was evacuated and then filled with a flowing stream of 20% oxygen in argon at ambient temperature. As noted previously, the oxygen acts to remove carbonaceous impurities from the freshly pretreated surface (*22*). For unmodified gold, only a single clearcut Raman band at 260 cm^{-1}, due to the metal-adsorbate stretch of residual adsorbed chlorine from the pretreatment procedure (*24*), is observed under these conditions. The surface was then heated to 475 K for about 1 min in hydrogen to reduce any remaining surface impurities. (This procedure was followed for all surfaces considered here. The resulting surface state is subsequently referred to as "reduced." The SERS activity survived such temperature excursions, at least to 550 K.)

The spectra in Figs. 1a and 2a, spanning the frequency regions 200–750 cm^{-1} and 750–1250 cm^{-1}, respectively, were obtained immediately (within ca. 5 s) following exposure of this reduced gold surface to the laser beam in a pure argon stream. In addition to the 260-cm^{-1} band referred to above, the latter spectrum displays a broad background at frequencies above ca. 1100 cm^{-1}. This feature, which extends to about 1600 cm^{-1}, grows progressively with prolonged exposure to the laser beam. (Moving the laser spot subsequently to a fresh region of the surface yields a similar time-dependent behavior). Most likely, then, this broad feature arises from the photochemical production of carbonaceous deposits, formed from organic impurities in the argon stream (cf. Ref. (*25*)). The use of the spectrograph-CCD arrangement allowed us to minimize the deleterious influence of this process, since spectra could be obtained sufficiently rapidly after exposing the surface to the laser beam (within ca. 10 s) so that only relatively weak 1100 to 1600-cm^{-1} features were obtained. The spectra reported here were generally obtained by using these tactics. Nevertheless, the formation of such carbonaceous deposits is attenuated greatly, even at room temperature, by including an oxidant such as oxygen in the argon feed (*22*).

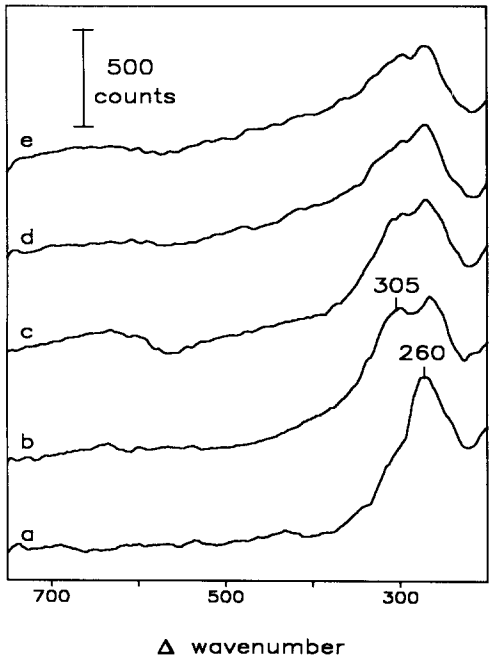

FIG. 1. SER spectra observed in the low frequency region (200–750 cm^{-1}) for a reduced gold surface exposed to various flowing argon mixtures: (a) pure argon, (b) 2% SO_2, (c) 20% O_2 + 5 % CO + 2% SO_2, (d) after the addition of 10 μl of water to the feed in (c), and (e) after removing SO_2 from the feed in (d). The total gas flow rate was 100 cm^3 min^{-1}. Laser excitation was 20 mW at 647.1 nm; the integration time was 10 s.

Figures 1b and 2b show corresponding SER spectra obtained similarly, but for an argon stream that contains 2% sulfur dioxide. New SER features are clearly observable at 305 and 1135 cm^{-1}. Although the band intensities are independent of the sulfur dioxide partial pressure, the 1135-cm^{-1} feature is evident only in the presence of gas-phase sulfur dioxide. In contrast, the intensity of the 305-cm^{-1} band remains unchanged when sulfur dioxide is removed from the feed and upon evacuation of the chamber. It is removed, however, upon heating to 475 K.

Gas-phase sulfur dioxide has three funda-

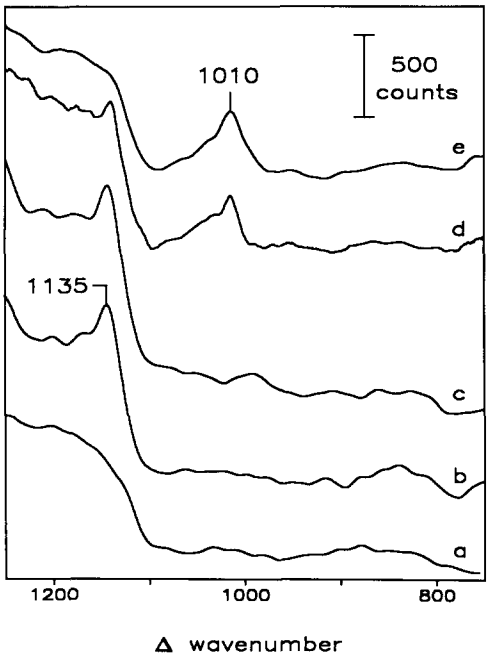

FIG. 2. As for Fig. 1, but in the S–O stretching region (750–1250 cm^{-1}).

mental vibrations: an O–S–O bending mode (δ) at 519 cm^{-1}, a symmetric S–O stretch (ν_s) at 1151 cm^{-1}, and an asymmetric S–O stretch (ν_a) at 1361 cm^{-1} (*26*). The stretching frequencies for coordinated sulfur dioxide depend on the binding configuration as well as on the identity of the coordinating metal (*27*). Two types of unidentate metal–ligand (M–L) coordination have been identified in S-bound transition metal–sulfur dioxide complexes which are associated with planar and pyramidal, or bent, configurations. The observed ranges of ν(SO) for the planar configuration are 1190–1300 cm^{-1} for ν_a and 1045–1140 cm^{-1} for ν_s; for the pyramidal configuration these ranges are 1115–1225 cm^{-1} for ν_a and 990–1065 cm^{-1} for ν_s. The ν(SO) values for sulfur dioxide coordinated via sulfur in twofold briding geometries have been observed from 1135 to 1240 cm^{-1} and 975 to 1085 cm^{-1} for ν_a and ν_s, respectively (*27, 28*). Sulfur dioxide complexes that are coordinated to a metal atom through both the sulfur and an oxygen atom (S,O-coordination) exhibit ν_a values from 1100 to 1160 cm^{-1} and ν_s from 850 to 950 cm^{-1} (*27, 28*). The present SER band observed at 1135 cm^{-1} can be assigned to an S–O stretch of adsorbed sulfur dioxide, although it is difficult to assign this ν(SO) band to either an asymmetric or symmetric mode. In the Raman spectrum of free sulfur dioxide, the observed intensity of the ν_s mode is much greater than that of the ν_a band (*26*). The band observed at 1135 cm^{-1} is therefore assigned tentatively to the ν_s of adsorbed sulfur dioxide, most likely in an S-bound planar configuration. The present SER spectra for adsorbed SO_2 differ significantly from reported EEL spectra obtained on Ag(110) (*9, 10*), Pd(100) (*11*), and Cu(100) (*13*) in that the latter yield a stronger ν_s and a weaker ν_a band having frequencies consistent with a pyramidal S-bound adsorbate structure (vide infra).

The present SER band at 305 cm^{-1} may also be associated with molecularly adsorbed SO_2, specifically the metal–sulfur (M–S) stretch. However, the retention of this band upon removal of gas-phase SO_2, contrasting the behavior of the 1135-cm^{-1} band, indicates that the origin of the former is probably different. Most likely, the 305-cm^{-1} band arises from the M–S stretch of adsorbed sulfur formed by SO_2 dissociative chemisorption. Vibrational frequencies reported for adsorbed atomic sulfur are 375 cm^{-1} on Pt(111) (*29*), 324 cm^{-1} on Cu(100) (*13*), and 290 to 305 cm^{-1} on Pd(100) (*11*).

Similar results were obtained when the gold surface was exposed to oxygen prior to dosing with sulfur dioxide or to a mixture of sulfur dioxide and oxygen. The presence of preadsorbed oxygen or oxygen in the gas phase therefore has little effect on the adsorption of sulfur dioxide on gold. The effect of added carbon monoxide was also examined since it is typically present in combustion processes. The results obtained are similar to those already discussed. As shown in Figs. 1c and 2c, the SER spectra recorded for a gold surface exposed to a mixture of 2% sulfur dioxide, 5% carbon monoxide,

and 20% oxygen in argon also exhibit similar vibrational bands at 305 and 1135 cm^{-1}.

The effect of added water vapor was also investigated. After the SER spectrum was obtained for a given feed composition, 10 μl of water was injected into the feed and spectra recorded every 10 sec. The presence of water resulted in no observable changes in the SER spectrum for a gold surface exposed to sulfur dioxide or to mixtures of sulfur dioxide with either oxygen or carbon monoxide separately. As shown in Fig. 2d, however, the addition of water to a feed containing sulfur dioxide, oxygen, *and* carbon monoxide yielded a band at 1010 cm^{-1} along with a decrease in the intensity of the 1135-cm^{-1} band. The 305-cm^{-1} band survives largely unchanged under these conditions. Unlike the 1135-cm^{-1} feature, the 1010-cm^{-1} band remains after removal of SO_2 from the feed (Fig. 2e) and also after evacuation. Nonetheless, the 1010-cm^{-1} feature could be removed irreversibly by heating the surface above 325 K.

Most likely, the 1010-cm^{-1} band arises from an oxidation product of SO_2, either sulfur trioxide or sulfate. Sulfur trioxide complexes exhibit symmetric and asymmetric S–O stretches in the ranges 930–990 cm^{-1} and 1000–1110 cm^{-1}, respectively (*9, 30*). Given that the symmetric SERS mode should be most intense, the 1010-cm^{-1} band has a higher frequency than expected for coordinated SO_3. Coordinated sulfate, however, commonly exhibits symmetric S–O stretches in the range ca. 900–1030 cm^{-1} (*10, 12, 30*), the highest frequencies being associated with unidentate coordination and the lowest with chelating bidentate binding. The asymmetric S–O stretches for coordinated sulfate range from ca. 1280 to 1035 cm^{-1} (*10, 12, 30*). We therefore tentatively assign the 1010-cm^{-1} band to adsorbed sulfate, most likely to the symmetric stretch of the unidentate coordinated form.

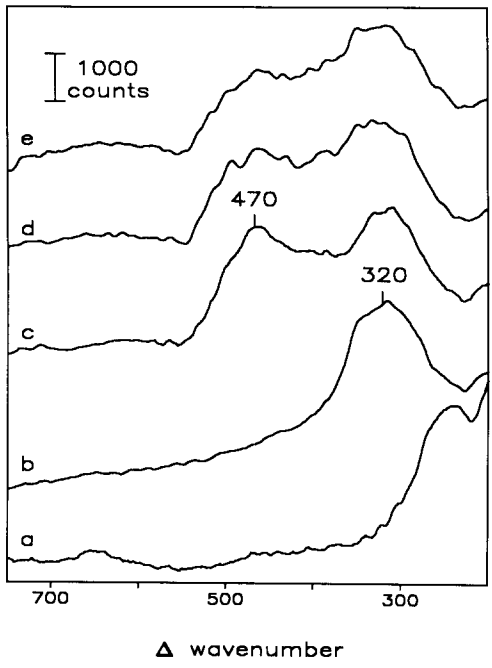

FIG. 3. SER spectra observed for a reduced platinum-coated gold surface exposed to various flowing argon mixtures: (a) pure argon, (b) 2% SO_2, (c) 20% O_2 + 5% CO + 2% SO_2, (d) after the addition of 10 μl of water to the feed in (c), and (e) after removing SO_2 from the feed in (d). The overlayer coverage was two equivalent monolayers; other conditions are as in the caption to Fig. 1.

Platinum-Coated Gold

The SER spectrum obtained for reduced platinum-coated gold surface in flowing argon (Figs. 3a, 4a), exhibits no distinct Raman bands; the Au–Cl stretch at 260 cm^{-1}, observed for unmodified gold surfaces, is only weak. Typical SER spectra obtained for a reduced platinum-coated gold surface exposed to a mixture of 2% sulfur dioxide in argon are shown in Figs. 3b and 4b. Raman bands are evident at 320, 940, and 1135 cm^{-1}. The intensities of these bands are independent of the sulfur dioxide partial pressure, although only the band at 320 cm^{-1} remains when sulfur dioxide is removed from the feed. Unlike the 305-cm^{-1} feature on unmodified gold, removal of the 320-cm^{-1} band required heating to 475 K in an oxygen atmosphere. Since the 320-cm^{-1} band is also upshifted significantly (15 cm^{-1}) compared to that on unmodified gold, it is assigned to the M–S stretch of sulfur ad-

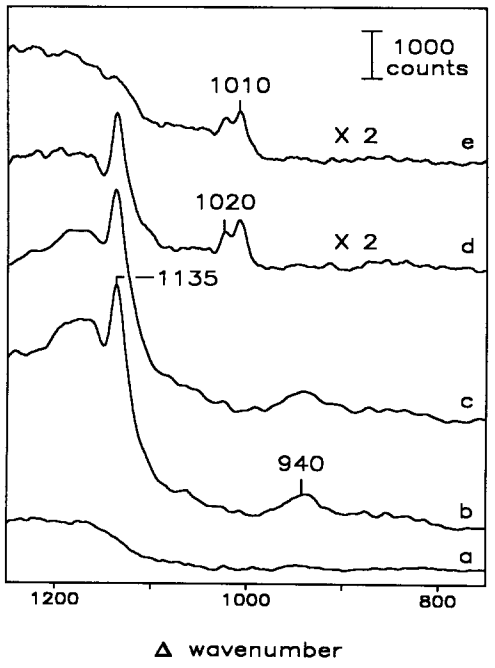

FIG. 4. As for Fig. 3, but in the S–O stretching region (750–1250 cm^{-1}).

sorbed on platinum rather than on residual gold sites. Following the arguments above, the band observed at 1135 cm^{-1} is assigned to ν(SO) of adsorbed sulfur dioxide. Although the observed intensity of the ν(SO) band at 1135 cm^{-1} is much greater for the platinum-coated surface than for unmodified gold, it is difficult to judge on this basis if the sulfur dioxide is adsorbed purely on platinum or additionally on residual gold sites. The frequency of the 940-cm^{-1} band is consistent with that expected for the symmetric stretch of adsorbed sulfur dioxide having S,O-coordination as well as similar modes for adsorbed sulfate or adsorbed sulfur trioxide (vide supra).

When sulfur dioxide is dosed on a platinum surface that has been exposed previously to oxygen or to mixtures of sulfur dioxide and oxygen, only the 320-cm^{-1} feature is evident, the bands at 940 and 1135 cm^{-1} not being observed. This contrasts the corresponding behavior of unmodified gold, where the ν(SO) band at 1135 cm^{-1} was observed under all conditions. The 1135-cm^{-1} band on platinum-coated gold therefore appears to arise primarily from SO_2 bonding to platinum rather than to residual gold sites.

The SER spectra for a platinum-coated gold surface exposed to mixtures of sulfur dioxide with carbon monoxide or carbon monoxide and oxygen are similar to those obtained for reduced platinum surfaces; Raman bands are evident at 320, 940, and 1135 cm^{-1} (Figs. 3c, 4c). In addition, there is a band observed at 470 cm^{-1} (Fig. 3c) which is assigned to the metal–carbon stretch, ν(PtC), for adsorbed carbon monoxide (*22*).

The effect of added water was similar to that obtained for unmodified gold surfaces; there was no observable change in the SER spectra with the addition of water to feeds of sulfur dioxide or to mixtures of sulfur dioxide with either oxygen or carbon monoxide. As for unmodified gold, however, if water is added to a feed of sulfur dioxide, carbon monoxide, and oxygen, two new bands are observed in the SER spectrum at 1010 and 1020 cm^{-1} (Fig. 4d). The intensity of the 1135-cm^{-1} band also decreases significantly and the 940-cm^{-1} feature is no longer evident. The bands at 1010 and 1020 cm^{-1} remain if sulfur dioxide is removed from the feed and are stable after evacuation (Fig. 4e). As before, these bands are tentatively assigned to the formation of adsorbed sulfate. Since the 1020-cm^{-1} band is absent on unmodified gold, it is assigned to ν(SO) of sulfate adsorbed on platinum. The 1010-cm^{-1} band is also attributed to a ν(SO) of adsorbed sulfate, but it is difficult to say if the band is due to sulfate adsorbed on gold or on platinum sites since a band is observed at the same frequency for unmodified gold. The intensity of this band is, however, about three times greater on the platinum-coated gold surface so the platinum is at least yielding more sulfate, even if some of it may be adsorbed on residual gold sites. The intensity of both the 1010- and 1020-cm^{-1} bands was seen to decrease as the surface temperature was increased above 300 K, virtually disappearing by 335 K. Neither band re-

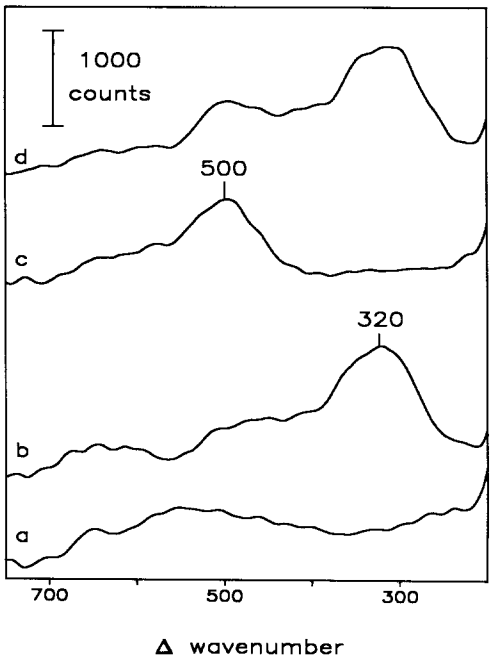

FIG. 5. SER spectra observed for reduced rhodium-coated gold surface exposed to various flowing argon mixtures: (a) pure argon, (b) 2% SO_2, (c) 20% O_2, (d) 20% O_2 + 2% SO_2. The overlayer coverage was three equivalent monolayers; other conditions are as in the caption to Fig. 1.

turned upon cooling the surface to room temperature.

Rhodium-Coated Gold

There are no clearcut Raman bands evident in the SER spectra for a reduced rhodium-coated gold surface in flowing argon (Fig. 5a). The addition of 2% sulfur dioxide to the argon feed results in a single band at 320 cm^{-1} (Fig. 5b); there is no evidence of a ν(SO) band at higher frequencies that would indicate the presence of adsorbed sulfur dioxide. The intensity of the 320-cm^{-1} band does not change if sulfur dioxide is removed from the feed or if the sample chamber is evacuated. As before, this feature is assigned to the metal-adsorbate stretch of adsorbed sulfur formed from the dissociative chemisorption of sulfur dioxide.

The SER spectrum for a rhodium surface that has been exposed previously to oxygen exhibits a band at 500 cm^{-1} (Fig. 5c); this has been assigned to the Rh–O stretch, ν(RhO), of adsorbed atomic oxygen (*22*). The addition of 2% sulfur dioxide to the argon feed results in the irreversible attenuation of the ν(RhO) feature and the appearance of the 320-cm^{-1} band (Fig. 5d). There is again no evidence of a ν(SO) stretch at 1135 cm^{-1}. Identical results were obtained with the addition of 2% sulfur dioxide to a feed of 20% oxygen in argon. This process was complete within 2 min after the introduction of sulfur dioxide into the feed. There was no change in the intensity of the band at 320 cm^{-1} as the surface was heated to 475 K. If the surface was held at this temperature in an oxygen atmosphere for several minutes, however, a gradual decrease in the 320-cm^{-1} band intensity was observed and the ν(RhO) band appeared.

The results obtained for rhodium surfaces exposed to feeds containing carbon monoxide were essentially the same as outlined above. The addition of sulfur dioxide to the feed results in a band at 320 cm^{-1} and bands attributed to adsorbed carbon monoxide, namely the Rh–C stretch at 465 cm^{-1}, decrease in intensity. There is again no evidence of a ν(SO) stretch at 1135 cm^{-1}. In contrast to the results obtained for gold and platinum-coated gold surfaces, the addition of water resulted in no observable changes in the SER spectrum for all of the feed mixtures studied.

Ruthenium-Coated Gold

The SER spectrum for a reduced ruthenium-coated gold surface in flowing argon is shown in Figs. 6a and 7a. The broadbands centered at 490 and 610 cm^{-1} have been assigned to adsorbed atomic oxygen and to more tightly bound oxide, respectively (*22*). In contrast to the other surfaces, heating the surface to 475 K in flowing hydrogen did not completely remove adsorbed oxygen from the ruthenium surface. (Holding the surface at 475 K for extended periods of time or

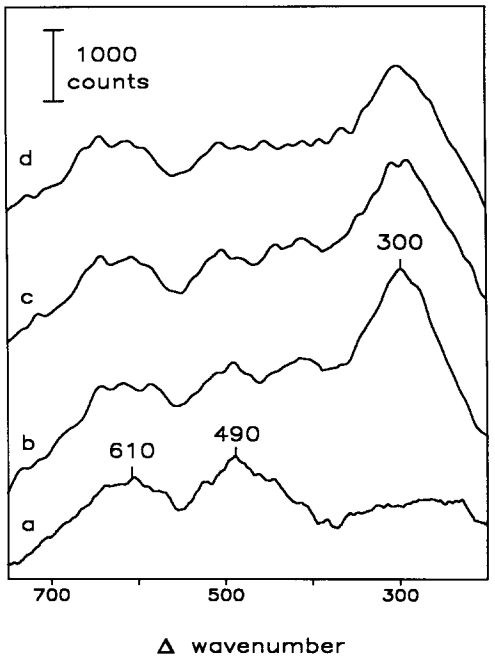

FIG. 6. SER spectra observed for a reduced ruthenium-coated gold surface exposed to various flowing argon mixtures: (a) pure argon, (b) 2% SO_2, (c) after the addition of 10 μl of water to 20% O_2 + 2% SO_2, (d) after heating the surface in (c) to 423 K in 20% O_2. The overlayer coverage was three equivalent monolayers; other conditions are as in the caption to Fig. 1.

increasing the temperature above this point resulted in an irreversible loss in the surface Raman enhancement.) The addition of sulfur dioxide to the feed results in a SER band at 300 cm^{-1} (Fig. 6b), as well as a barely discernible feature at 1135 cm^{-1} (Fig. 7b). There is also a decrease in the intensity of the 490-cm^{-1} Ru–O band with the addition of sulfur dioxide. The 1135-cm^{-1} band is assigned to the ν(SO) of adsorbed sulfur dioxide, although it cannot be determined if the adsorption is occurring on ruthenium or on gold since both the band frequency and intensity are similar to those obtained on unmodified gold. The 300-cm^{-1} band is assigned as before to the metal-adsorbate stretch of an adsorbed sulfur species formed from the dissociative chemisorption of sulfur dioxide. Virtually identical results were obtained with the addition of sulfur dioxide to feeds containing oxygen, carbon monoxide, or both oxygen and carbon monoxide.

The results obtained for ruthenium surfaces with the addition of water were somewhat different from those obtained for other surfaces. Although there was no change in the SER spectrum with the addition of water to a feed of just sulfur dioxide and argon, the addition of water to feeds containing both sulfur dioxide and oxygen, with and without carbon monoxide, results in a new band at 1030 cm^{-1} (Fig. 7c). As before, this band is assigned to ν(SO) of adsorbed sulfate. (Recall that for gold and platinum-coated gold surfaces, such bands were only observed with the addition of water to feeds containing sulfur dioxide, oxygen, and carbon monoxide.) The 1030-cm^{-1} feature is stable to evacuation. The band cannot be seen in spectra obtained at temperatures greater than 325 K, although it returns to its full intensity when the surface is cooled to

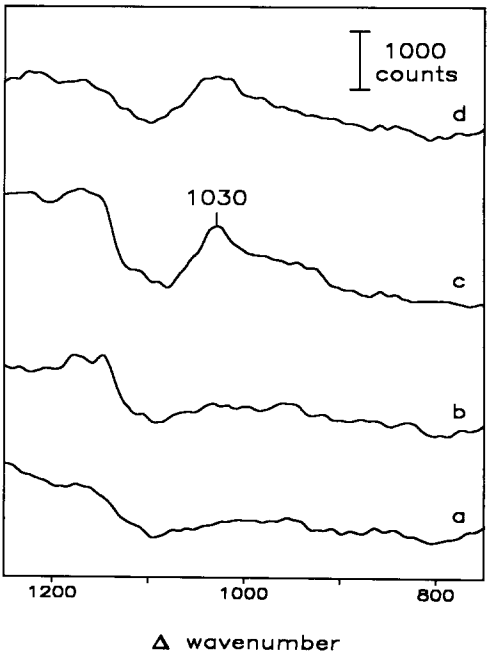

FIG. 7. As for Fig. 6, but in the S–O stretching region (750–1250 cm^{-1}).

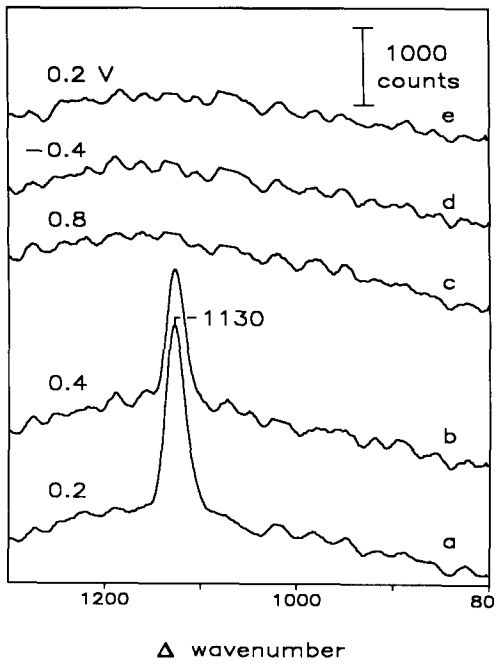

FIG. 8. Potential-dependent SER spectra in the S–O stretching region (800–1300 cm^{-1}) for an unmodified gold electrode in 0.5 *M* H_2SO_4 with dissolved SO_2. The potential was cycled from 0.2 to 1.5 V to −0.5 V and back at a rate of 0.1 V s^{-1}. Spectra were obtained sequentially at (a) 0.2, (b) 0.4, (c) 0.8, (d) −0.4, and (e) 0.2 V. Laser excitation was 40 mW at 647.1 nm; the integration time was 2 s.

room temperature (Fig. 6d). In contrast to similar bands observed on gold and platinum, then, the species associated with this band is not removed readily under these conditions.

Electrochemical Behavior

Potential-dependent SER spectra were obtained for aqueous solutions of sulfur dioxide, primarily in 0.1 *M* $HClO_4$ + 50 m*M* $HClO_4$. The electrolyte was sparged with SO_2 for ca. 10–20 s. Between ca. −0.1 V and 0.4 V vs saturated calomel electrode (SCE) on unmodified gold, the SO_2 is essentially stable to reduction and oxidation, respectively (cf. Ref. (*31*)). Under these conditions, a band was observed at 1130 cm^{-1} on unmodified gold (Fig. 8a), similar to that seen in the corresponding gas-phase environment (Fig. 2b). Sweeping the potential positive of ca. 0.4 V (at 0.01–0.1 V s^{-1}) results in the disappearance of this band (Fig. 8b,8c), which does not return after the potential sweep is reversed so as to traverse the original values (Fig. 8d).

Sweeping the potential negative of −0.1 V yields a band at ca 300 cm^{-1} (Fig. 9e). As before, this feature can be attributed to the surface-adsorbate stretch for atomic sulfur; in this case, however, the sulfur appears only upon electroreduction of sulfur dioxide. After reversing the potential at −0.5 V and sweeping back positive beyond −0.2 V, the 300-cm^{-1} band is attenuated and new features appear at 220 and 460 cm^{-1} (Fig. 9f). The 460- and 220-cm^{-1} bands can be attributed to S–S stretch and bending modes, respectively, for polysulfides (*32, 33*); these are presumably formed by sulfide electrooxidation (*34–36*). These assignments are supported by the observation of identical spectral changes during the elec-

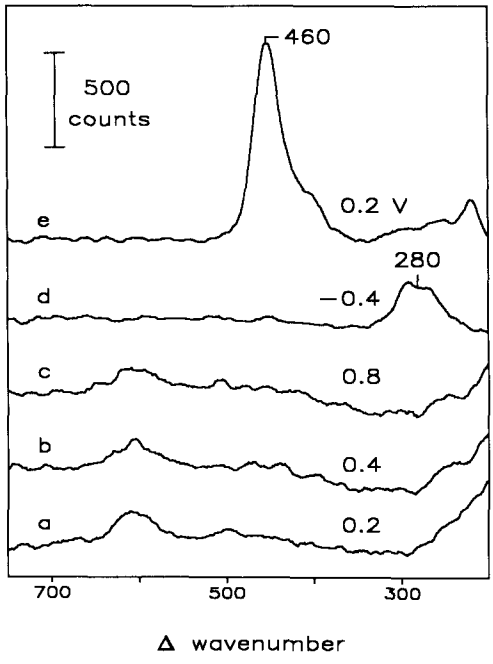

FIG. 9. As for Fig. 8, but in the low frequency region (200–750 cm^{-1}).

trooxidation of sulfide on unmodified gold under these conditions (in the acidic electrolyte employed, the added sulfide is present as H_2S). The surface must be held at 1.5 V for several seconds to remove completely the band at 460 cm^{-1}, so the adsorbed polysulfide is slowly oxidized. Although it can be reduced to sulfide at potentials negative of −0.4 V, polysulfides immediately reform on the surface when the potential returns positive.

The voltammetric response obtained for a platinum-coated gold electrode in the presence of dissolved sulfur dioxide in 0.1 *M* $NaClO_4$ + 50 m*M* $HClO_4$ is similar to that of an unmodified gold surface; SO_2 is oxidized at potentials positive of 0.4 V and is reduced negative of −0.1 V. The potential-dependent SER spectra on the Pt-coated surface, however, are significantly different. If SO_2 was introduced into the solution with the electrode held at −0.1 to 0 V (i.e., so as to avoid surface electrooxidation), a broadband at ca. 1100 cm^{-1} is obtained (Fig. 10a), attributed to adsorbed SO_2. Sweeping the potential to more positive values (ca. 0.2 V and higher) yields a diminution of this feature along with the appearance of bands centered at 1065 and 930 cm^{-1} (Fig. 10b–10d). The latter features survive even at far positive potentials. The 930-cm^{-1} band is similar to that observed for SO_2 on platinum-coated gold in the gas phase (Fig. 4b). Most likely, both the 1065- and 930-cm^{-1} bands refer to oxidation products from adsorbed SO_2, either SO_3 and/or sulfate. Sweeping the potential back to negative values results in the partial reappearance of the 1100-cm^{-1} feature (Fig. 10e). The potential-dependent SER spectra on Pt-coated gold in the 200 to 500-cm^{-1} region at negative potentials, where SO_2 reduction occurs, are comparable to those observed on unmodified gold.

Similarly to platinum, the spectra obtained on rhodium-coated gold electrodes are sensitive to the prior state of the surface. At potentials, −0.1 to 0 V, where the surface is largely reduced (i.e., is oxide-free),

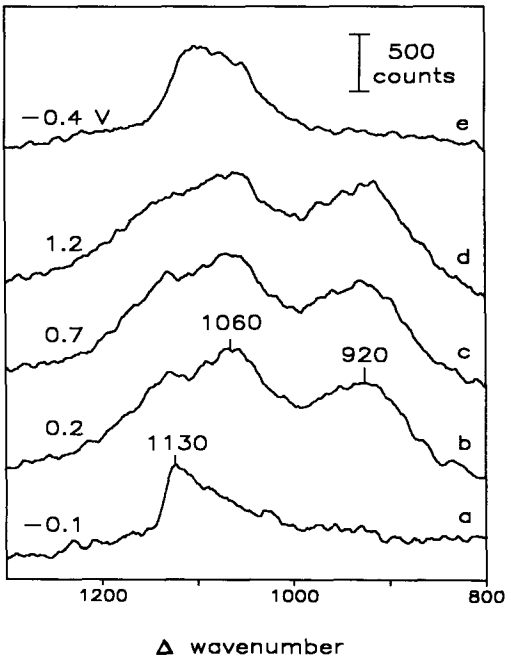

FIG. 10. Potential-dependent SER spectra for a platinum-coated gold electrode in 0.5 *M* H_2SO_4 with dissolved SO_2. Spectra were obtained sequentially at (a) −0.1, (b) 0.2, (c) 0.7, (d) 1.2, and (e) −0.4 V. The overlayer coverage was two equivalent monolayers; other conditions are as in the caption to Fig. 8.

addition of SO_2 yields a band centered at ca. 1100 cm^{-1}, again indicative of molecular SO_2 adsorption. Sweeping the potential positive yields a diminution of this feature along with the appearance of bands at 960 and 1080 cm^{-1}, again presumably due to the formation of adsorbed SO_3 and/or sulfate. The behavior at negative potentials, upon SO_2 reduction, is similar to that on gold and platinum. On ruthenium-coated gold electrodes, dosing with SO_2 at −0.1 V yields a weak feature at 1120 cm^{-1}, which gives way to a band at 1015 cm^{-1} by ca. 0.4 V. Initial SO_2 dosing at more positive potentials, however, yields no significant features in the 900–1150 cm^{-1} region, although the 600-cm^{-1} band due to the ruthenium–oxygen stretch grows in intensity under these conditions. Again, the SERS behavior on ruthenium at negative potentials is similar to that observed on the other surfaces.

No clearcut ν(SO) bands due to adsorbed sulfate were obtained at the present electrochemical surfaces in the presence of solution sulfate anions. While this finding certainly does not eliminate sulfate species as a likely assignment of the 1060- to 1080-cm^{-1} features formed upon SO_2 electrooxidation on platinum and rhodium, it nevertheless is indicative of a distinctly different mode of surface binding in the latter case.

DISCUSSION

The present results indicate, not surprisingly, that the nature of the SO_2 binding along with the extent of dissociation and adsorbate oxidation is sensitive to the nature of the metal–gas surface. At least on unmodified gold and on the platinum overlayer in the gas phase, significant molecular adsorption of SO_2 occurs, as evidenced by the ca. 1135-cm^{-1} band. The virtual absence of this feature on rhodium and ruthenium in the gas phase, signaling the paucity of molecularly adsorbed SO_2, can be understood partly from the greater extent of dissociative chemisorption to form adsorbed sulfur, as discerned from the ca. 300-cm^{-1} band, and from the prevalence of adsorbed oxygen on these easily oxidized surfaces, even under "reducing" conditions. The role of the latter factor is readily seen, for example, in the attenuation of the 1135-cm^{-1} SERS band for SO_2-dosed platinum surfaces that had undergone prior exposure to oxygen.

Broadly speaking, the appearance of molecularly adsorbed SO_2, as gleaned from the 1100–1150 cm^{-1} region, is largely similar at the corresponding metal-aqueous interfaces, at least at potentials where SO_2 is stable to oxidation or reduction. One difference, however, is the appearance of bands at 1100–1135 cm^{-1} for reduced rhodium and ruthenium electrodes, that are weak or absent at the corresponding "reduced" surfaces in the gas phase. This dissimilarity, however, is not surprising since adsorbed oxygen (or oxide) can more readily be removed in the electrochemical environment by appropriate potential control.

In a similar vein, an interesting difference between the two environments is the common observation of dissociative SO_2 chemisorption to form sulfur on the metal–gas surfaces, as reflected in the appearance of the ca. 300-cm^{-1} band on unmodified gold as well as the transition metals, along with the 1100 to 1135-cm^{-1} band for molecularly adsorbed SO_2. At the electrochemical interfaces, however, the production of adsorbed sulfur can largely be avoided by keeping the potential positive of ca. -0.1 V. This behavioral dissimilarity illustrates a fundamental difference between the gas-phase and electrochemical systems: for the latter, the occurrence of adsorbate oxidation or reduction (in this case reductive dissociation) is influenced by the electrode potential which can be controlled externally. In the former case, the potential (i.e., the work function) is determined by the nature of the metal and the adsorbate surface composition.

Another behavioral difference between the gas-phase and electrochemical environments is that SO_2 reduction and subsequent reoxidation in the latter case yields adsorbed polysulfides as discerned from the 460- and 220-cm^{-1} bands; no such chemistry occurs in the former systems. Most likely, the polysulfide formation involves the reoxidation of dissolved sulfide, which is obviously absent in the gas-phase environment. A detailed examination of the sulfide/polysulfide electrochemical system by means of time-resolved SERS is underway, and will be reported elsewhere.

As mentioned above, dissociative SO_2 chemisorption yielding sulfur adlayers has also been observed on several metal surfaces in uhv, along with the common appearance of molecular adsorption. Regarding the latter, the present occurrence of SO_2 bound in a planar configuration, as inferred from the SERS 1100 to 1135-cm^{-1} features, differs somewhat from the behavior on metal-

uhv surfaces at temperatures below 200 K, as obtained from EELS data. Thus bands assigned to ν_s for molecularly adsorbed SO_2 have been reported at 1005 cm^{-1} on Ag(110) (*9*), at 1035 cm^{-1} on Pd(100) (*11*), and at 978 cm^{-1} on Cu(100) (*13*). Based on these frequencies, as noted above, the SO_2 was interpreted as bridging in a pyramidal, or bent, configuration. There are apparently no previous reports of SO_2 adsorption at metal–gas interfaces at ambient temperatures, presumably due to the high gas pressures required to avoid thermal desorption. Both the small ν_s frequency shift upon adsorption and the ready thermal desorption of the molecularly adsorbed SO_2 under the present conditions, however, point to a likely presence of weak surface-adsorbate interactions.

An interesting question raised by the present results is the manner in which SO_2 undergoes surface oxidation to form sulfate and possibly SO_3. One curious aspect is that SO_2 oxidation on both the platinum and unmodified gold surfaces in the gas phase requires the presence of water along with O_2 *and* CO. The role of CO could well be manifold. For platinum, the appearance of SO_2 adsorption itself in the presence of oxygen also requires CO; the last species could partly remove tightly bound oxygen (by forming CO_2 or by competitive adsorption), enabling SO_2 binding and subsequent oxidation to take place. In addition, the adsorbed CO may well be more readily displaced than atomic oxygen, thereby enabling sulfate adsorption to occur. Somewhat surprising in this regard, however, is the behavior of the ruthenium surface in that sulfate formation upon the addition of water and O_2 occurs on this metal even in the absence of carbon monoxide.

Although adsorbed species resulting from SO_2 oxidation are also observed in the corresponding aqueous electrochemical environments, there are significant behavioral differences. Thus the band frequencies of the oxidized species formed on platinum and rhodium, ca. 1060–1080 cm^{-1}, are significantly higher than those at the surface–gas interfaces. In addition, no adsorbed oxidation products are detected at the unmodified gold-aqueous interface. In general, these differences are not surprising, especially given that solubility in the aqueous solution phase will inevitably affect retention of the adsorbed products in the electrochemical systems.

The EELS vibrational properties of the sulfate formed by oxidation of adsorbed SO_2 with oxygen on uhv surfaces also differs significantly from those observed at the present metal–gas interfaces. For example, the sulfate formed on Ag(110) at temperatures above 475 K yields a strong ν_s band at 910 cm^{-1} and weaker (presumably ν_a features) at 1070 and 1275 cm^{-1} (*10*). These differences can be understood from the bidentate sulfate coordination apparently involved in the uhv systems (*10–12*), as compared with the unidentate binding most likely occurring in the present systems.

Together with the results of a companion paper concerned with NO, CO, and oxygen adsorption (*22*), we believe that the present results testify to the value of SERS for monitoring the vibrational properties of adsorbates on transition-metal as well as noble-metal surfaces in the gas phase, even at ambient pressures and elevated temperatures. The recent advent of CCD technology enables surface Raman spectra to be obtained for a variety of adsorbates, even under "weak SERS" conditions (such as occurring with thicker overlayers) within a few seconds.

Of particular interest to us in this connection are the prospects of coupling such time-resolved SERS observations with transient (or "non-steady state") kinetic measurements for heterogeneous catalytic systems obtained simultaneously in the flow reactor system. We have pursued analogous coupled real-time SERS-electrochemical measurements for some time (*37*), and these studies are especially viable now with CCD

detection. We hope to report on experiments involving combined SERS-heterogeneous catalytic kinetic measurements in the near future.

ACKNOWLEDGMENTS

This work is supported in part by grants from the National Science Foundation to M.J.W. (CHE-88-18345) and to C.G.T. (CBT-86-11176).

REFERENCES

1. Satterfield, C. N., "Heterogeneous Catalysis in Practice," p. 295. McGraw–Hill, New York, 1980.
2. Brundle, C. R., and Carley, A. F., *Faraday Discuss. Chem. Soc.* **60,** 51 (1975).
3. Furuyama, M., Kishi, K., and Ikeda, S., *J. Electron Spectrosc. Relat. Phenom.* **13,** 59 (1978).
4. Ku, R. C., and Wynblatt, P., *Appl. Surf. Sci.* **8,** 250 (1981).
5. Bonzel, H. P., and Ku, R., *J. Chem. Phys.* **59,** 1641 (1973).
6. Astegger, S., and Bechtold, E., *Surf. Sci.* **122,** 491 (1982).
7. Kohler, U., and Wassmuth, H.-W., *Surf. Sci.* **117,** 668 (1982).
8. Rovida, G., and Pratesi, F., *Surf. Sci.* **104,** 609 (1981).
9. Outka, D. A., Madix, R. J., Fisher, G. B., and DiMaggio, C. L., *Langmuir* **2,** 406 (1986).
10. Outka, D. A., Madix, R. J., Fisher, G. B., and DiMaggio, C. L., *J. Phys. Chem.* **90,** 4051 (1986).
11. Burke, M. L., and Madix, R. J., *Surf. Sci.* **194,** 223 (1988).
12. Burke, M. L., and Madix, R. J., *J. Phys. Chem.* **92,** 1974 (1988).
13. Leung, K. T., Zhang, X. S., and Shirley, D. A., *J. Phys. Chem.* **93,** 6164 (1989).
14. Outka, D. A., and Madix, R. J., *Surf. Sci.* **137,** 242 (1984).
15. Dorain, P. B., von Raben, K. U., Chang, R. K., and Laube, B. L., *Chem. Phys. Lett.* **84,** 405 (1981).
16. Matsuta, H., and Hirokawa, K., *Appl. Spectrosc.* **43,** 239 (1989).
17. Matsuta, H., and Hirokawa, K., *Appl. Surf. Sci.* **27,** 482 (1987).
18. Seki, H., *J. Electron Spectrosc. Relat. Phenom.* **39,** 289 (1986).
19. Leung, L.-W. H. and Weaver, M. J., *J. Am. Chem. Soc.* **109,** 5113 (1987).
20. Leung, L.-W. H., and Weaver, M. J., *Langmuir* **4,** 1076 (1988).
21. Gao, X., and Weaver, M. J., to be published.
22. Wilke, T., Gao, X., Takoudis, C. G., and Weaver, M. J., *Langmuir*, in press.
23. Gao, P., Gosztola, D., Leung, L.-W. H., and Weaver, M. J., *J. Electroanal. Chem.* **233,** 211 (1987).
24. Gao, P., and Weaver, M. J., *J. Phys. Chem.* **290,** 4057 (1986).
25. Tsang, J. C., Demuth, J. E., Sanda, P. N., and Kirtley, J. R., *Chem. Phys. Lett.* **76,** 54 (1980).
26. Herzberg, G., "Molecular Spectra and Molecular Structure II," p. 285. Van Nostrand, Princeton, NJ, 1945.
27. Kubas, G. J., *Inorg. Chem.* **18,** 182 (1979).
28. Ryan, R. R., Kubas, G. J., Moody, D. C., and Eller, P. G., *Struct. Bonding* **46,** 47 (1981).
29. Koestner, R. J., Salmeron, M., Kollin, E. B., and Gland, J. L., *Surf. Sci.* **172,** 668 (1986).
30. Nakamoto, K., "Infrared and Raman Spectra of Inorganic and Coordination Complexes," p. 250. Wiley, New York, 1986.
31. Samec, Z., and Weber, J., *Electrochim. Acta.* **20,** 403,413 (1975).
32. Janz, G. J., Downey, J. R., Jr., Roduner, E., Wasilczyk, G. J., Coutts, J. W., and Elvard, A., *Inorg. Chem.* **15,** 1759 (1976).
33. Janz, G. J., Roduner, E., Coutts, J. W., Downey, J.R., Jr., *Inorg. Chem.* **15,** 1751 (1976).
34. Hamilton, I. C., and Woods, R., *J. Appl. Electrochem.* **13,** 783 (1983).
35. Buckley, A. N., Hamilton, I. C., Woods, R., *J. Electroanal. Chem.* **216,** 213 (1987).
36. Lezna, R. O., de Tacconi, N. R., Arvia, A. J., *J. Electroanal. Chem.* **283,** 319 (1990).
37. For example, see Gao, P., Gosztola, D., and Weaver, M. J., *Anal. Chim. Acta.* **212,** 201 (1988).